

Gravitational collapse in anti de Sitter space

David Garfinkle*

*Department of Physics, University of Guelph, Guelph, Ontario, Canada N1G 2W1
and Perimeter Institute for Theoretical Physics, 35 King Street North, Waterloo Ontario, Canada N2J 2W9*

A numerical and analytic treatment is presented here of the evolution of initial data of the kind that was conjectured by Hertog, Horowitz and Maeda to lead to a violation of cosmic censorship. That initial data is essentially a thick domain wall connecting two regions of anti de Sitter space. The evolution results in no violation of cosmic censorship, but rather the formation of a small black hole.

I. INTRODUCTION

A longstanding issue in general relativity is that of cosmic censorship: the question of whether the singularities formed in gravitational collapse are hidden inside black holes. This old question was given a new twist by Hertog, Horowitz and Maeda[1] who conjectured that cosmic censorship can be violated in certain spacetimes that are asymptotically anti de Sitter. The proposed counterexample consists of a matter model, an initial data set and an argument that the evolution of that initial data gives rise to a singularity that cannot be hidden inside a black hole.

The matter model is a scalar field with a potential with two minima below zero. The potential is chosen so that the system just barely satisfies the positive mass theorem. The initial data is essentially a spherically symmetric, thick domain wall that interpolates between regions of the two anti de Sitter spaces corresponding to the two potential minima. The data is chosen so that for an inner region of radius R , the mass is proportional to R . Since anti de Sitter space is unstable, it is argued in[1] that the evolution of this initial data will result in a singularity in the central region and further that for sufficiently large R the mass of the spacetime will not allow the formation of a black hole large enough to cover the singularity.

The nature of this issue was changed when Dafermos[2] proved that any singularities formed in the evolution of the system of [1] cannot be visible to observers at infinity. Thus if the arguments of [1] were correct, then the singularity would extend to infinity. In other words the entire space would collapse in a Big Crunch.

However, various authors[3, 4, 5, 6] have expressed misgivings about the arguments of [1] (including the authors of [1] in [7]). The authors of [3, 4, 7] express doubts over the assumption in [1] that the central region can be well approximated as a spacetime that is homogeneous but not anti de Sitter. The authors of [5, 6] raise the possibility that the wall might move outward indefinitely.

It is not clear how to settle this issue using analytical means. Therefore it makes sense to perform numerical simulations of the evolution of the initial data of [1] and find the outcome. Such a simulation was reported in[3] for $R = 7$ with the result that a small black hole formed rather than a naked singularity. However, this did not resolve the issue since it was argued in[1, 7] that “sufficiently large” R means $R \geq 600$.

In this work we simulate the evolution of the initial data of[1] for large R . Here too, the result is the formation of a small black hole, not a naked singularity. Though the results are numerical, the most important properties of this system can be understood analytically using the properties of perturbations of anti de Sitter space.

Sec. II presents the relevant equations and numerical method. Sec. III contains a treatment of perturbations of anti de Sitter space. Results of the numerical simulations are presented in Sec. IV and conclusions in Sec. V.

II. EQUATIONS AND NUMERICAL METHODS

The system to be studied is a spherically symmetric scalar field ϕ with a potential V . The appropriate equations are therefore the Einstein-scalar equations:

$$G_{ab} = \nabla_a \phi \nabla_b \phi - g_{ab} (\frac{1}{2} \nabla^c \phi \nabla_c \phi + V) \quad (1)$$

$$\nabla_a \nabla^a \phi = \frac{\partial V}{\partial \phi} \quad (2)$$

*Electronic address: david@physics.uoguelph.ca

(Here we are using units where $8\pi G = 1$). We use polar-radial coordinates for the metric which puts it in the form

$$ds^2 = -\alpha^2 dt^2 + a^2 dr^2 + r^2 (d\theta^2 + \sin^2\theta d\varphi^2) \quad (3)$$

It is helpful to define the quantities X and Y given by $X \equiv \partial\phi/\partial r$ and $Y \equiv (a/\alpha)\partial\phi/\partial t$. Then equation (2) yields the following evolution equation for Y

$$\frac{\partial Y}{\partial t} = \frac{1}{r^2} \frac{\partial}{\partial r} \left(r^2 \frac{\alpha}{a} X \right) - \alpha a \frac{\partial V}{\partial \phi} \quad (4)$$

while Einstein's equation yields the following equations which are used to find the metric components α and a .

$$\frac{\partial a}{\partial r} = \frac{a(1-a^2)}{2r} + \frac{1}{4} r a (X^2 + Y^2 + 2a^2 V) \quad (5)$$

$$\frac{\partial}{\partial r} \ln(a\alpha) = \frac{r}{2} (X^2 + Y^2) \quad (6)$$

Einstein's equation also provides an evolution equation for a . Defining the quantity $\mathcal{C} \equiv \partial a/\partial t - r\alpha XY/2$ then it follows from Einstein's equation that \mathcal{C} vanishes. We will use this as a code check. That is, equations (4-6) are used to simulate the evolution of the system and then the results of that simulation are checked by seeing that \mathcal{C} converges to zero.

The numerical method used is essentially that of reference[3]. That is spatial derivatives are replaced by centered differences for unequally spaced points, while time evolution is done using the iterated Crank-Nicholson (ICN) method.[8] The equations are stabilized using Kreiss-Oliger dissipation.[9]

The spacing of the grid points is different from that of[3]. Define the coordinate ρ by $r \equiv \tan \rho$. Though the coordinate r is used in all equations, we choose a grid of points that is equally spaced in ρ .

The potential used is that of reference[1]

$$V(\phi) = -3 + 50\phi^2 - 81\phi^3 + k\phi^6 \quad (7)$$

where the constant k is chosen so that the system just barely satisfies the positive mass theorem. The initial data is chosen to minimize the contribution of the potential to the total mass. Here the minimum is found over all field configurations that are in the true vacuum at $r = 0$ and the false vacuum for $r \geq R$. This leads to an ordinary differential equation for ϕ that is solved using a shooting method as described in[3]. For our purposes, an important property of the solution is that in the central region $\phi \propto r^\beta$ where $\beta = (\sqrt{409} - 3)/2 \approx 8.6$.

III. ANTI DE SITTER PERTURBATIONS

We now consider the behavior of the central region as a perturbation of anti de Sitter space. The initial data in the central region has $\phi \propto r^\beta$ where $\beta \approx 8.6$. Thus the scalar field is very small. Keeping only terms up to linear order in ϕ we find that equations (5-6) yield $\alpha^2 = a^{-2} = 1 + r^2$, while equation (4) becomes

$$-\frac{\partial^2 \phi}{\partial t^2} + \frac{1+r^2}{r^2} \frac{\partial}{\partial r} \left(r^2 [1+r^2] \frac{\partial \phi}{\partial r} \right) - 100(1+r^2)\phi = 0 \quad (8)$$

Defining $\psi \equiv r\phi$ and $\rho \equiv \tan^{-1}r$ we obtain

$$-\frac{\partial^2 \psi}{\partial t^2} + \frac{\partial^2 \psi}{\partial \rho^2} - \frac{102\psi}{\cos^2 \rho} = 0 \quad (9)$$

Provided that the spatial and temporal variation of ψ is sufficiently large, the last term in this equation can be neglected yielding for an ingoing wave $\psi = f(t + \rho)$ or

$$\phi = \frac{1}{r} f(t + \tan^{-1}r) \quad (10)$$

We will later see from the numerical results that for large walls, the last term in equation (9) is negligible. However, the reason for this is easy to understand analytically: Define a "coordinate thickness" Δr of the wall as follows: Let Δr be the amount that r varies as ϕ varies from 10% to 90% of its maximum value. Correspondingly define $\Delta \rho$. Since the initial data depends only on r/R , it follows that $\Delta r \propto R$. However, this means that for large walls (*i.e.* those

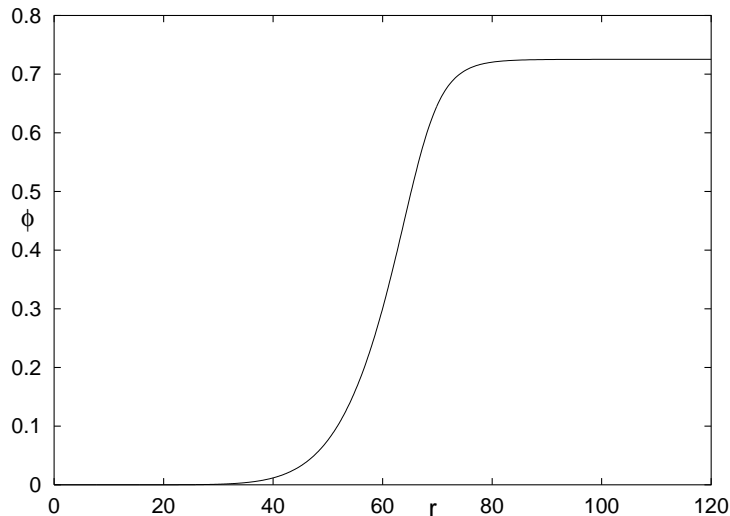


FIG. 1: the scalar field ϕ at $t = 0$. $R = 100$ and $N = 256000$

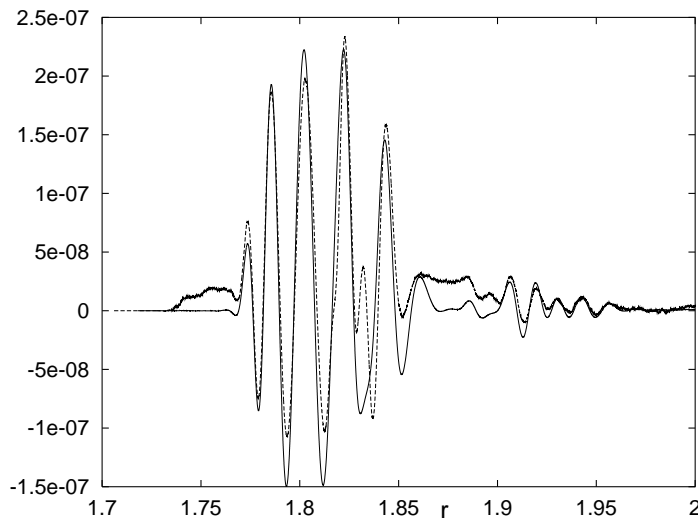


FIG. 2: the constraint at $t = 0.5$ for $R = 100$ at two different resolutions: \mathcal{C} for $N = 256000$ (solid line) and $8\mathcal{C}$ for $N = 512000$ (dashed line)

with $R \gg 1$) we have $\Delta\rho \propto R^{-1}$. Thus viewed as a function of ρ , the initial data is essentially zero in the central region and then steeply increases to its maximum value in a narrow region near $\pi/2$. The evolution of such initial data is a narrow wave packet that propagates inward.

Once the wave packet reaches values of $r \ll 1$, the difference between anti de Sitter space and Minkowski space becomes irrelevant. The subsequent behavior of the wave packet then depends on whether it will shrink to a size smaller than its Schwarzschild radius or whether it will disperse.

IV. NUMERICAL RESULTS

All runs were done in double precision on a Sun Blade 2000. Let $N + 1$ be the number of spatial grid points. We first present results for $R = 100$. Figure 1 shows the initial data for ϕ . The evolution of this initial data produces very narrow wave packets; so all plots of the evolution of the initial data will be confined to the range of r where the wave packet is present.

Figure 2 shows the result of a convergence test of the code. Here, the system is evolved to a time of 0.5 in two

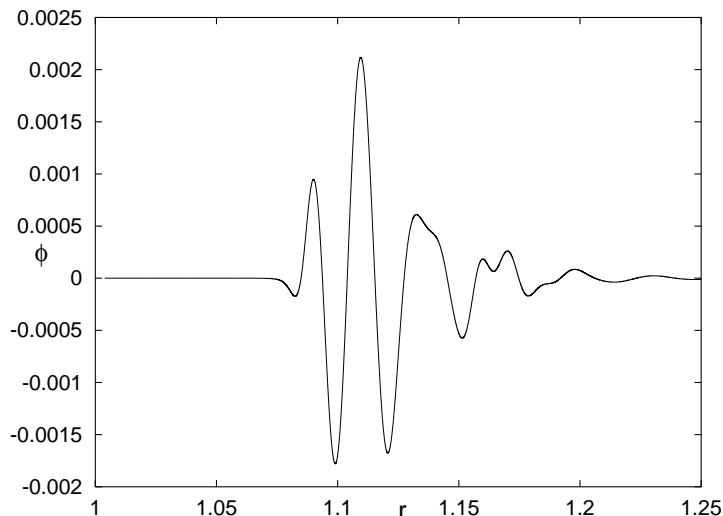


FIG. 3: the scalar field ϕ at $t = 0.731$. $R = 100$ and $N = 256000$

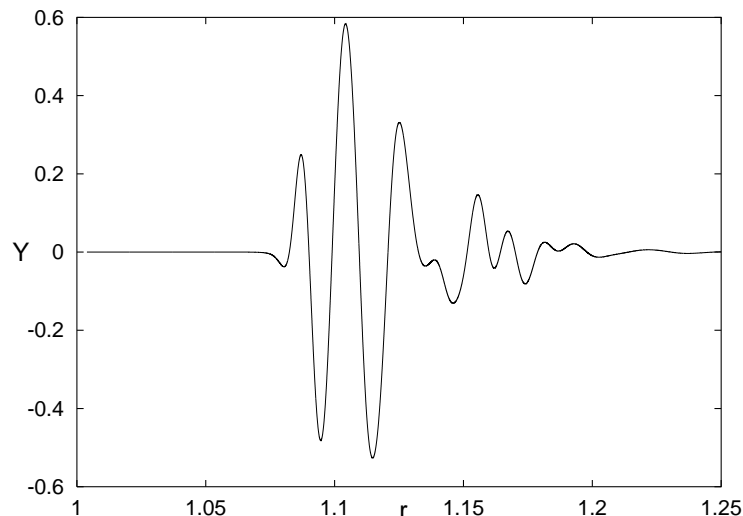


FIG. 4: Y at $t = 0.731$. $R = 100$ and $N = 256000$

different runs: one with $N = 256000$ and the other with $N = 512000$. What is plotted in the figure is the quantity \mathcal{C} for the $N = 256000$ run (solid line) and $8\mathcal{C}$ for the $N = 512000$ run (dashed line). The result shows that the constraint converges to zero at third order. This is a bit surprising, since from the finite difference techniques used one would expect the code to be only second order convergent. However, it may be that for this type of ingoing wavepacket the leading part of the truncation error for the constraint vanishes.

Figures 3-9 show the results of a run with $N = 256000$. Figures 3 and 4 show respectively ϕ and Y for the evolution of the initial data to a time $t=0.731$. Note that $\partial\phi/\partial t \sim 570\phi$. Therefore, the last term in equation (9) is negligible, justifying the expression in equation (10). Figure 5 shows $r\phi$ as a function of $t + \rho$ for two times: $t = 0.2$ (solid line) and $t = 0.4$ (dashed line). These curves agree, showing that equation (10) is a good approximation for this part of the evolution. In contrast, figure 6 shows ϕ as a function of r for these two times. Here one sees two well separated wave packets.

Figures 7, 8 and 9 show respectively ϕ , Y and a at the final time. Here the final time, which is slightly less than $\pi/2$, is chosen by having the simulation end when the maximum value of a reaches 3.5 corresponding to $2m/r = 0.92$. The reason for this is that the coordinate system used here breaks down when a trapped surface forms and that breakdown is signalled by a becoming large where the trapped surface forms. Thus figure 9 indicates that a trapped surface forms at $r \approx 0.0056$, while figures 7 and 8 indicate that the region of high curvature is contained within this

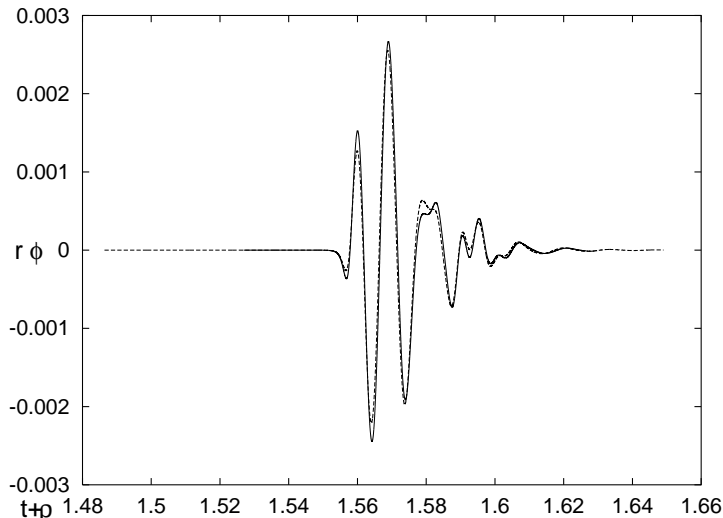


FIG. 5: $r\phi$ as a function of $t + \rho$ at $t = 0.2$ (solid line) and $t = 0.4$ (dashed line). $R = 100$ and $N = 256000$

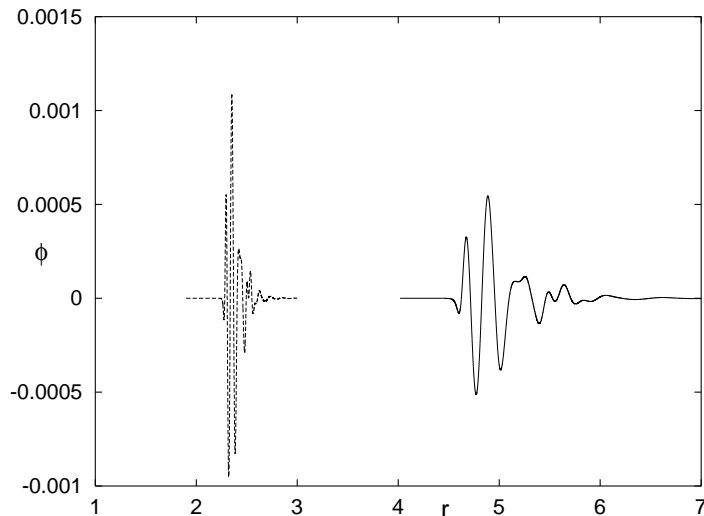


FIG. 6: ϕ as a function of r at $t = 0.2$ (solid line) and $t = 0.4$ (dashed line). $R = 100$ and $N = 256000$

trapped surface. Thus the result of the evolution of the initial data with $R = 100$ is a small black hole.

These numerical results for $R = 100$ do not directly address the conjecture of [1] which is for $R \geq 600$. However, a wall with $R = 600$ leads to a wavepacket that is much more narrow in ρ and therefore requires far more resolution and thus much more computer memory and time for a simulation that evolves all the way to black hole formation. Instead we will evolve such initial data for a comparatively short time that is nonetheless long enough to (i) verify that the result is a narrow wavepacket and (ii) show that the wavepacket has enough energy that its collapse will result in a black hole. Figures 10 and 11 show the results of a run with $R = 600$ and $N = 1024000$ evolved to a time of $t = 0.1$. Here ϕ is plotted in figure 10 and Y is plotted in figure 11. Note that the result is a narrow wavepacket centered near $r = 10$, just as one would expect from the treatment of section III. Also note that $\partial\phi/\partial t \sim 3.8 \times 10^3 \phi$. For comparison, figures 12 and 13 give respectively ϕ and Y for a run with $R = 100$ and $t = 0.1$. ($N = 256000$ for this run). Note that the $R = 600$ wavepacket has a higher amplitude and shorter wavelength than the $R = 100$ wavepacket. Thus the $R = 600$ wavepacket has more energy within a shell of smaller thickness than the $R = 100$ wavepacket. Since a black hole forms from the further evolution of the $R = 100$ case, it then follows that the evolution of the more energetic wavepacket of the $R = 600$ case will also result in the formation of a black hole.

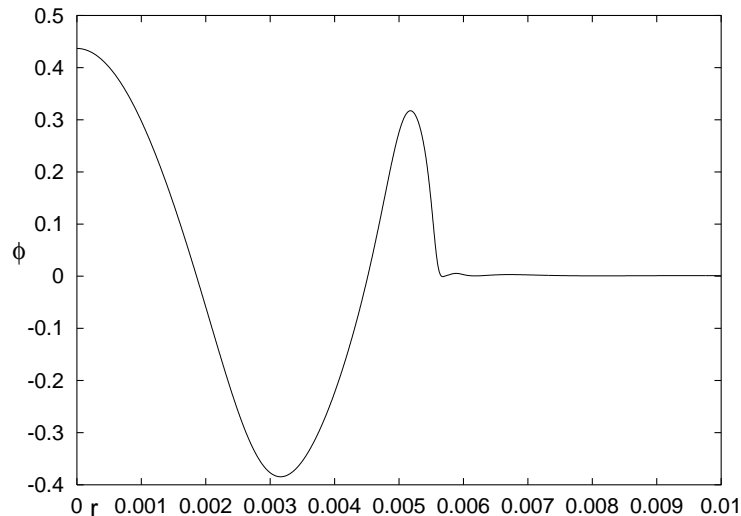


FIG. 7: ϕ at the final time. $R = 100$ and $N = 256000$

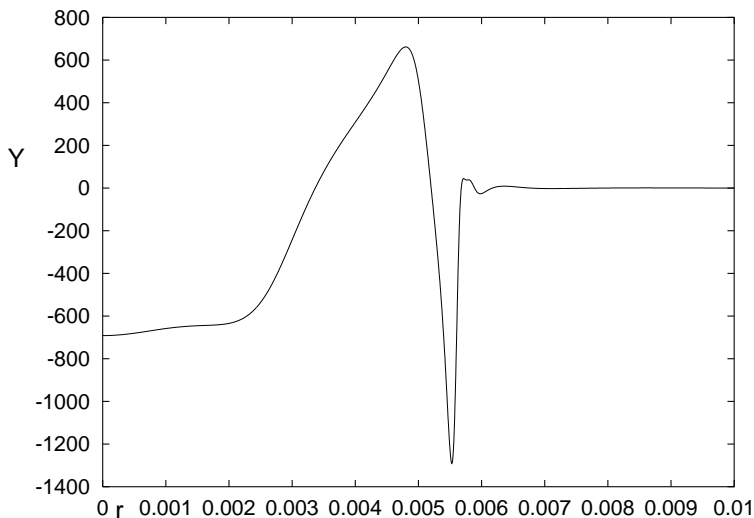


FIG. 8: Y at the final time. $R = 100$ and $N = 256000$

V. CONCLUSIONS

We then see that the initial data of [1] when evolved, does not form a naked singularity, but instead forms a small black hole. In hindsight, the reason for this is clear. The authors of [1] assumed, correctly, that the evolution of the central region could be described for a while by a perturbation of anti de Sitter space. However, they also assumed, incorrectly, that the perturbation is homogeneous. In the initial data $\phi \propto r^\beta$ where $\beta \approx 8.6$. Thus the initial amplitude for the homogeneous part of the perturbation is so small as to be negligible. Instead, the perturbation comes from the wall, *i.e.* the transition region between the two vacua. In the ρ coordinate, this transition region is very narrow (especially for walls with large R). Therefore the evolution of this initial data is a narrow wavepacket that propagates inward. In the course of the evolution, the wavepacket becomes sufficiently concentrated that it is no longer well described by perturbation theory. The numerical simulation then shows that the wavepacket collapses to form a small black hole. Thus cosmic censorship is not violated by the evolution of the initial data given in [1].

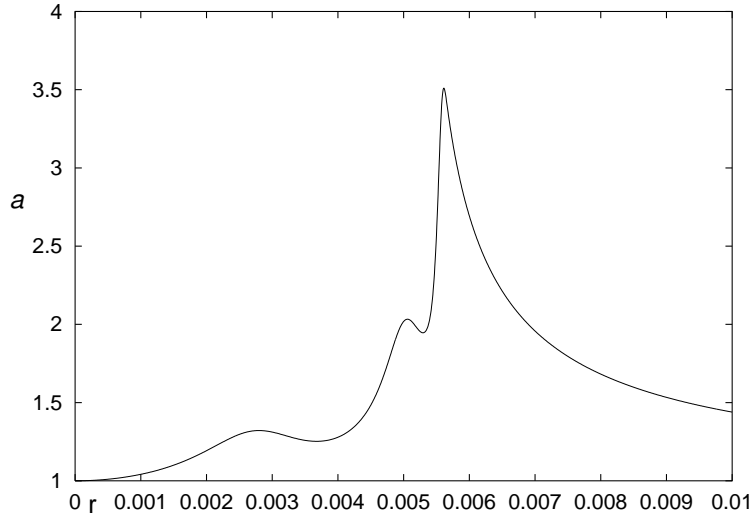


FIG. 9: a at the final time. $R = 100$ and $N = 256000$

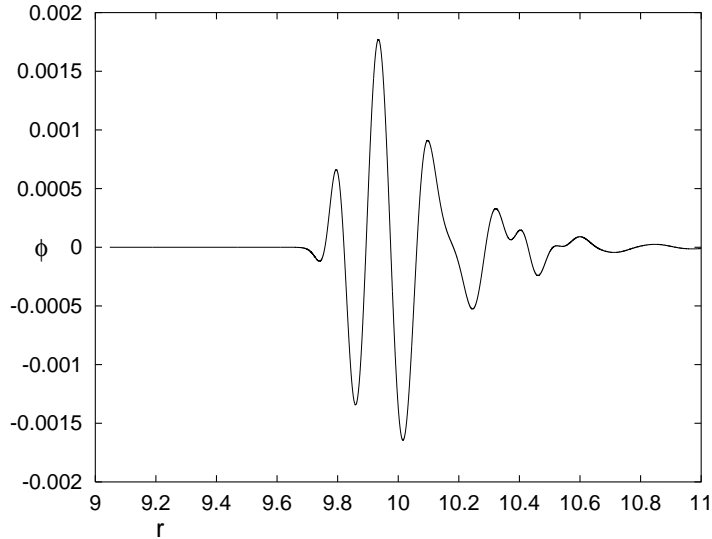


FIG. 10: ϕ at $t = 0.1$. $R = 600$ and $N = 1024000$

VI. ACKNOWLEDGMENTS

I would like to thank Gary Horowitz for helpful discussions. This work was partially supported by a grant from NSERC.

-
- [1] T. Hertog, G. Horowitz and K. Maeda, Phys. Rev. Lett. **92**, 131101 (2004)
 - [2] M. Dafermos, gr-qc/0403033
 - [3] D. Garfinkle, Phys. Rev. **D69**, 124017 (2004)
 - [4] V. Hubeny, X. Liu, M. Rangamani and S. Shenker, hep-th/0403198
 - [5] M. Alcubierre, J. Gonzalez, M. Salgado and D. Sudarsky, gr-qc/0402045
 - [6] M. Alcubierre, J. Gonzalez, M. Salgado and D. Sudarsky, gr-qc/0406070
 - [7] T. Hertog, G. Horowitz and K. Maeda, gr-qc/0405050
 - [8] M. Choptuik, in *Deterministic Chaos in General Relativity*, edited by D. Hobill, A. Burd and A. Coley (Plenum, New York, 1994), pp. 155-175

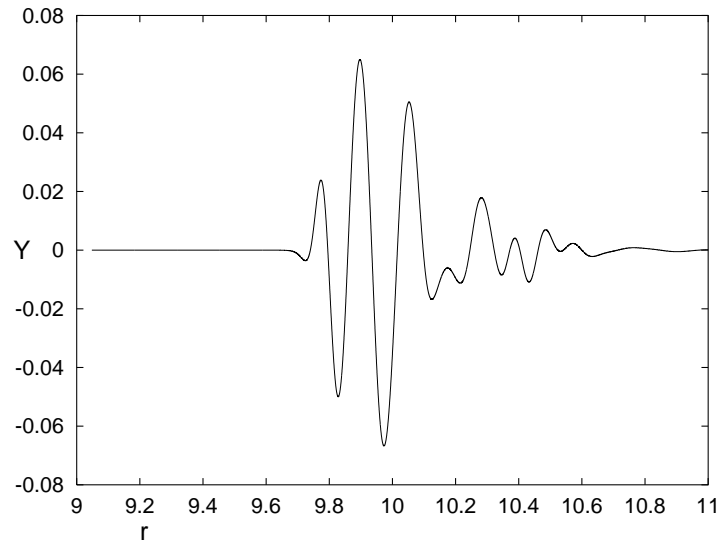


FIG. 11: Y at $t = 0.1$. $R = 600$ and $N = 1024000$

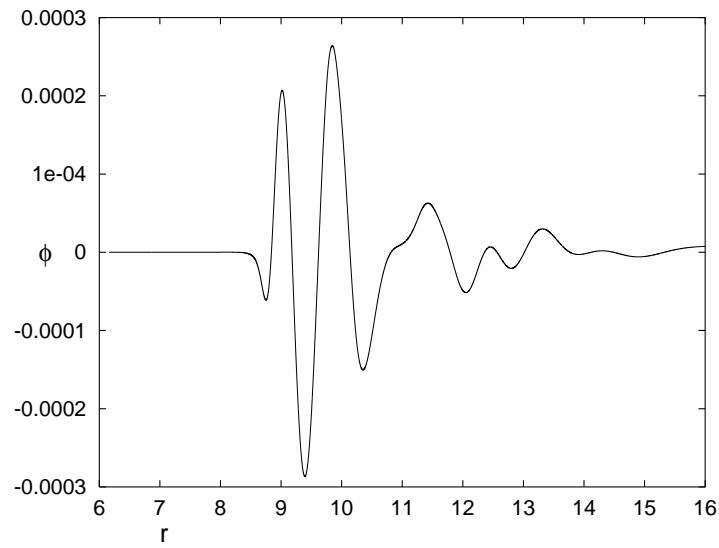


FIG. 12: ϕ at $t = 0.1$. $R = 100$ and $N = 256000$

- [9] H. Kreiss and J. Olinger, Methods for the Approximate Solution of Time Dependent Problems, Global Atmospheric Research Programme, Publication Series No. 10 (1973)

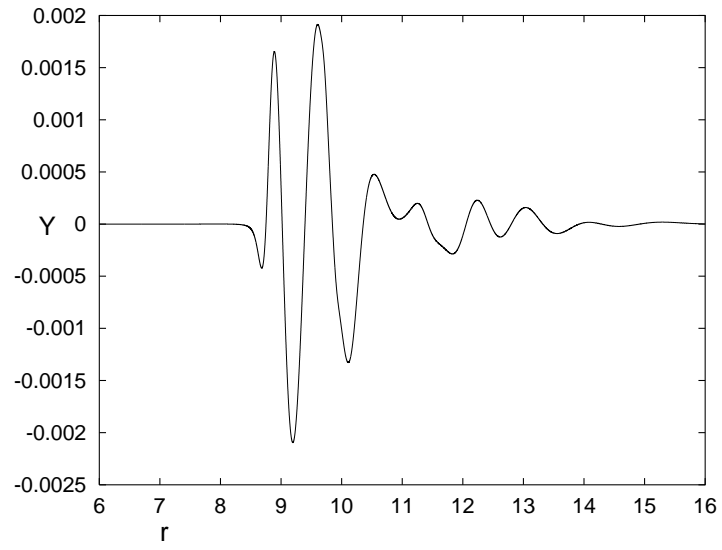


FIG. 13: ϕ at $t = 0.1$. $R = 100$ and $N = 256000$